Models and Technologies

Molecular Cancer Therapeutics

Sprague Dawley *Rag2*-Null Rats Created from Engineered Spermatogonial Stem Cells Are Immunodeficient and Permissive to Human Xenografts

Fallon K. Noto[1], Valeriya Adjan-Steffey[2], Min Tong[3], Kameswaran Ravichandran[4], Wei Zhang[1], Angela Arey[1], Christopher B. McClain[5], Eric Ostertag[2], Sahar Mazhar[6], Jaya Sangodkar[7], Analisa DiFeo[7], Jack Crawford[1,2], Goutham Narla[1,7], and Tseten Y. Jamling[1,2]

Abstract

The rat is the preferred model for toxicology studies, and it offers distinctive advantages over the mouse as a preclinical research model including larger sample size collection, lower rates of drug clearance, and relative ease of surgical manipulation. An immunodeficient rat would allow for larger tumor size development, prolonged dosing and drug efficacy studies, and preliminary toxicologic testing and pharmacokinetic/pharmacodynamic studies in the same model animal. Here, we created an immunodeficient rat with a functional deletion of the Recombination Activating Gene 2 (*Rag2*) gene, using genetically modified spermatogonial stem cells (SSC). We targeted the *Rag2* gene in rat SSCs with TALENs and transplanted these *Rag2*-deficient SSCs into sterile recipients. Offspring were genotyped, and a founder with a 27 bp deletion mutation was identified and bred to homozygosity to produce the Sprague-Dawley *Rag2* -*Rag2*^{tm1Hera} (SDR) knockout rat. We demonstrated that SDR rat lacks mature B and T cells. Furthermore, the SDR rat model was permissive to growth of human glioblastoma cell line subcutaneously resulting in successful growth of tumors. In addition, a human KRAS-mutant non–small cell lung cancer cell line (H358), a patient-derived high-grade serous ovarian cancer cell line (OV81), and a patient-derived recurrent endometrial cancer cell line (OV185) were transplanted subcutaneously to test the ability of the SDR rat to accommodate human xenografts from multiple tissue types. All human cancer cell lines showed efficient tumor uptake and growth kinetics indicating that the SDR rat is a viable host for a range of xenograft studies.
Mol Cancer Ther; 17(11); 2481–9. ©2018 AACR.

Introduction

Preclinical research and drug discovery rely heavily on *in vitro* systems and animal models for safety and efficacy studies. However, *in vitro* and animal models do not always accurately predict human metabolism and toxicity (1–5). As a result, there have been cases in which a drug was deemed safe or efficacious in rodent studies, but which failed in clinical trials in humans (6–9). Immunodeficient mouse models of human cancer have paved the way for studying cancer biology, genomics, effects on cancer growth kinetics, propensity for metastasis, and treatment response. A plethora of genetically immunodeficient mouse models, with varying immune phenotypes, exist for such studies (10). However, drug efficacy testing and downstream analysis such as pharmacokinetic (PK)/pharmacodynamic (PD) studies are limited because of inconsistent or poor tumor engraftment, high variability in tumor growth kinetics, and limited tumor growth potential. As a result, a significantly large number of mice are used for drug efficacy screening in order to achieve a cohort of animals with tumors of similar size and similar tumor growth kinetics for treatment. We explored whether these cell lines might grow more consistently in a versatile *in vivo* model such as the immunodeficient rat.

The laboratory rat remains the favored species for toxicology research because of its relative physiologic similarity to humans (11–14). The metabolism and PK properties of drugs in rats are similar to humans compared with mice. All toxicology and safety profiling of drugs is performed in rats, whereas efficacy studies are conducted primarily in mice models due to a lack of appropriate

[1]Hera BioLabs Inc., Lexington, Kentucky. [2]Transposagen Biopharmaceuticals Inc., Lexington, Kentucky. [3]Poseida Therapeutics Inc., San Diego, California. [4]University of Colorado, Denver, Colorado. [5]Icahn School of Medicine at Mount Sinai, New York, New York. [6]Case Western Reserve University, Cleveland, Ohio. [7]The University of Michigan, Ann Arbor, Michigan.

Note: Supplementary data for this article are available at Molecular Cancer Therapeutics Online (http://mct.aacrjournals.org/).

F.K. Noto, V. Adjan-Steffey, G. Narla, and T.Y. Jamling contributed equally to this article.

Corresponding Author: Tseten Y. Jamling, Hera Biolabs, 2277 Thunderstick Drive Suite 500, Lexington, KY 40505. Phone: 888-337-9836; E-mail: yeshi@herabiolabs.com

doi: 10.1158/1535-7163.MCT-18-0156

SCID-rat models. Data quality for drug development would be much improved if all the relevant data sets are generated in the same model.

Due to the large size of the rats, tumors can be grown to nearly 10 times the volume (or double the diameter) allowed in the mouse (15, 16). Rats have 10 times the blood volume of mice. Therefore, rats can accommodate multiple blood samplings from the same test animal at different time points for blood cancer efficacy assessment, clinical pathology profiling, and PK sampling. Because the rat is the preferred model for toxicology and safety testing, a rat with human cancer would allow for a combination of chemotherapy efficacy, PK, and preliminary toxicology testing all in one animal, thereby greatly reducing the number of animals needed while improving the quality of data generated.

In order to generate cancer xenograft models or "humanize" a tissue in the rodent by replacing endogenous cells with human cells or ectopically transplanting human tissues, the animal must be immunodeficient to inhibit rejection of the xenogeneic cells. Although many immunodeficient mouse models exist with differing capabilities for accepting human cells (10), very few rat models can engraft human cells (17, 18). The nude rat (RNU; NIH-*Foxn1*^{rnu}) is one such model that is completely devoid of T cells but has limited capacity for human cell engraftment because it still has a normal repertoire of B and natural killer (NK) cells (19). Several studies have demonstrated that the nude mouse is superior in its ability to engraft and support the growth of human cancers compared with the nude rat and that there is an increased incidence of tumor regression in the nude rat, likely due to its age-dependent changes in immune competence (20–22). Data from studies with several different immunodeficient mouse models suggest that mice in which both B and T cells are absent have a better propensity for supporting human cell engraftment and growth (23–28). Therefore, we have created a genetically immunodeficient rat which completely lacks B cells and has a severely reduced population of mature T cells.

Although targeted genetic modification of the laboratory mouse has been possible since the first isolation of mouse embryonic stem cells (29, 30), targeted gene knockouts and knockins have not been described in rats until recently. New gene-editing technologies such as TALENs and the CRISPR/Cas9 systems have now made targeted genetic modifications possible in the rat. We used *Xanthomonas* TALE Nuclease (XTN) to create a mutation in *Rag2* (Recombination Activating Gene 2) which is critical for V(D)J recombination, and its deletion disrupts maturation of B and T cells of the immune system (31, 32). Rat spermatogonial stem cells (SSC) were targeted, which have recently been described as an alternative to genetic manipulation of embryos in rats (33). These modified SSCs can assimilate into the testes of sterile males and give rise to normal offspring, allowing germline transmission of the genetic modification of interest in one generation.

Here, we report the generation of a Sprague-Dawley *Rag2* knockout (SDR) rat characterized by a loss of mature B cells and severely reduced T cells compared with wild-type Sprague Dawley rats. We demonstrate that these immunodeficient rats are permissive for human cancer xenografts with high efficiency and desirable uniformity in tumor growth profiles. Our data suggest that the SDR rat may be a viable novel model in which to study human cancers and may also be useful for transplantation of various other human cells and tissues.

Materials and Methods

Editing spermatogonial genome

All animal experiments were approved and met guidelines set forth by the University of Kentucky's Institutional Animal Care and Use Committee. Rat spermatogonial line SD-WT2 (Dr. Kent Hamra's lab, University of Texas Southwestern) was propagated in Spermatogonial Medium (SG) and cryopreserved in SG-freezing medium, as previously described (34). To generate *Rag2* mutants, spermatogonia were expanded to passage 16 (from cryopreserved passage 13 stocks) in fresh SG medium before collecting for nucleofection with *Rag2*-XTNs. Note that 10 μg total DNA of *Rag2*-XTN plasmids was added to 3×10^6 SSCs suspended in 100 μL Nucleofection Solution L (Amaxa) and subjected to nucleofection using settings A020 on the Nucleofector (Amaxa). After transfection, spermatogonia were subjected to 75 μg/mL G418 treatment for 20 days following a 7-day recovery and cryopreserved until transplantation.

Prior to transplantation, G418-selected spermatogonia were verified for carrying the desired mutation and correct karyotype. Genomic DNA was harvested from about 50,000 G418-selected spermatogonia and the targeted locus amplified. This pool of amplicons was TOPO cloned, and a 96-well plate of clones was sequenced for analysis to confirm disruption of the *Rag2* gene. Another cohort of nucleofected spermatogonia was sent to IDEXX BioResearch laboratories for karyotype analysis.

Immunocytochemistry

SD-WT2 spermatogonia at passage 16 were also subjected to immunocytochemistry to verify expression of SSC marker *Plzf* (ZBTB16). Spermatogonia were plated on cover slips in a 24-well plate. 3T3 cells were plated on uncoated cover slips, mouse embryonic fibroblast (MEF) feeders on gelatin-coated cover slips, SSCs cocultured with MEFs on laminin, and gelatin coated cover slips. Plated cells were washed twice with SG medium and fixed with 4% PFA for 7 minutes, and washed 3 times with PBS. They were then permeabilized with PBS plus 0.1%(v/v) TritonX-100 for 15 minutes and washed 3 times with PBS. Blocking reagent (11096176001; Roche) dissolved in Maleic acid was applied for 2 hours, followed by a 20-hour incubation at room temperature with 1 μg/mL of mouse anti-*Plzf* (OP128L; Calbiochem) in blocking reagent. Slides were washed 3 times with TBST to remove unbound IgG and incubated with 4 μg/mL Alexa Fluor 596 donkey anti-mouse IgG (A21203; Invitrogen), as the secondary antibody, in PBS containing 5 μg/mL Hoecsht33342 for 40 minutes at room temperature. Slides were washed 3 times with TBST and finished with Fluoromount (F4680; Sigma) for observation under fluorescent microscope.

Transplantation of modified spermatogonia

G418-selected spermatogonia were thawed and transplanted within 3 hours of thawing into Busulfan-treated, Dazl-deficient male Sprague Dawley rats as previously described (35, 36). Briefly, *Dazl*-deficient males were injected intraperitoneally with 12 mg/kg busulfan. Twelve days later, G418-resistant donor rat spermatogonia were thawed from cryopreserved stock, resuspended in ice-cold SG medium, and loaded into injection needles at concentration 3×10^5 cells/50 μL. The entire 50 μL volume was injected into the seminiferous tubes of anesthetized rats by retrograde injection. Transplanted males were subsequently bred to wild-type females 70 to 81 days later.

Screening for SDR rats

Total genomic DNA was extracted from pups born from *Dazl*-deficient males transplanted with modified spermatogonia. The targeted *Rag2* locus was PCR-amplified from the gDNA with *Rag2*_NHEJ-Fwd (GAGAAGGTGTCTTACGGTTCTATG) and *Rag2*_NHEJ-Rev (GCAGGCTTCAGTTTGAGATG) primers. The PCR product was purified and subjected to MseI digestion, and the digestion product was analyzed via gel electrophoresis with a 1% agarose gel for disruption of the targeted MseI restriction site. PCR amplicons that failed to be completely digested by MseI restriction enzyme were TOPO cloned, and 6 clones were sequenced to identify the sequence of the alleles in that sample.

FACS analysis of immune cells

To detect T, B, and NK cells in SDR rats, flow cytometric analysis was performed on splenocytes and thymocytes using a BD LSRII (BD Biosciences) flow cytometer. Spleen and thymus were collected in FACS buffer (BD Pharmingen, 554656). The tissues were homogenized and passed through a 70 μm cell strainer to remove clumps. Red blood cells were lysed by incubating with ACK Lysing Buffer (Quality Biological, #118-156-721) for 10 minutes at room temperature. Cells were stained with fluorophore-labeled antibodies at a final concentration of 25 μg/mL in 20 μL volume for 20 minutes. Antibodies used were Goat anti-rat IgM-APC (Stem Cell Technologies, #10215), FITC Mouse anti-rat CD45R (BD Pharmingen, #561876), FITC Mouse Anti-Rat CD8b (BD Pharmingen, #554973), APC Mouse Anti-Rat CD4 (BD Pharmingen, #550057), and FITC Mouse Anti-Rat CD161a (BD Pharmingen, #561781).

Transplantation of human cancer cell lines

Cell culture. Human glioblastoma cell line U87MG Red FLuc (Perkin Elmer, BW124577) was a gift from Dr. Bjoern Bauer at the University of Kentucky, human non–small cell lung cancer (NSCLC) cell line H358 (bronchioalveolar carcinoma, mutant KRAS) was a gift from Dr. Goutham Narla at the Case Comprehensive Cancer Center, Cleveland, OH, human ovarian carcinoma cell line OV81 obtained from high-grade serous ovarian cancer patient's patient-derived xenograft (PDX) tumor and human endometrioid cancer cell line OV185 obtained from a recurrent endometrioid patient's PDX tumor were a gift from Dr. Analisa DiFeo at the Case Comprehensive Cancer Center, Cleveland, OH. U87MG cells were grown in Eagle's Minimum Essential Medium with L-Glutamine (ATCC, #30-2003), Sodium Pyruvate (Gibco, #11360-070), FBS, and Non-Essential Amino Acids (Gibco, #11140-050). H358 cell lines were cultured in Advanced RPMI 1640 Medium (Gibco #12633-012) supplemented with 10% FBS (Atlanta Biologicals, # S12450) and 1% penicillin and streptomycin solutions (Cat# 15140-122, Thermo Fisher). OV81 and OV185 were grown in DMEM (Gibco, #10566-016) supplemented with 10% FBS (Atlanta Biologicals, # S12450) and 1% penicillin and streptomycin solutions (Cat# 15140-122, Thermo Fisher). All the cells were grown in a humidified incubator at 37° C with 5% CO_2. Cell lines were tested for Mycoplasma using the MycoAlert Mycoplasma detection Kit (Cat# LT07; Lonza). Experiments were performed within 6 to 8 cell passages after thaw.

Tumor xenografts. For transplantation, 1×10^6 U87MG cells, 1×10^6, 5×10^6, or 10×10^6 H358 cells, and 2×10^6 OV81 cells and OV185 cells for each animal were resuspended in 250 μL sterile 1xPBS (Gibco, #14190-144). Immediately prior to injection, 250 μL 10 mg/mL Geltrex (Gibco, #A14132-02) was added to the cell suspension for a final Geltrex concentration of 5 mg/mL. The cell/Geltrex suspension was injected subcutaneously into the hindflank. Tumor diameter was measured using digital calipers (Fisher, #14-648-17) 3 times a week. Tumor volume was calculated as $(L \times W^2)/2$ (37), where width and length were measured at the longest edges.

Immunohistochemistry of tumors

Tumors were excised and fixed in 10% neutral-buffered formalin for 48 hours. Tissue was processed, paraffin-embedded, and sectioned by the University of Kentucky Imaging Core Facility. Standard 5 μm sections were collected. Sections were stained with Harris' hematoxylin (Sigma, #HHS128) and Eosin (Sigma, #318906) for basic histology. Human cells were visualized by staining with an antibody that recognizes a protein found in all human mitochondria (mouse anti-human mitochondria antibody, clone 113-1; EMD Millipore, #1273). Chromogenic staining was performed by using biotinylated goat-anti mouse (Vector Labs, #BA-9200), then Vectastain Elite ABC HRP Reagent, R.T.U. (Vector Labs, #PK-7100), and developed using Pierce DAB substrate kit (Thermo Fisher, #34002). In some cases, sections were counterstained with Harris' hematoxylin to visualize nuclei. Images were taken using a Zeiss Palm Laser Microbeam Microscope in the University of Kentucky Imaging Core Facility.

Results

Rag2 knockout rat SSCs

XTNs (38, 39) were used to create a pool of spermatogonia in which about 3% of the cells contained disruptions in the *Rag2* gene. *Rag2* has a single coding exon. XTNs targeting a MseI restriction site near the start of this coding exon were nucleofected into SD-WT2 SSCs derived from wild-type Sprague-Dawley rat (*Hsd: Sprague-Dawley SD;* Harlan, Inc.). The location of the XTN-binding sites and PCR primers for genotyping are shown in Fig. 1A. Total genomic DNA was extracted from transfected spermatogonia clusters. The targeted locus was PCR amplified, TOPO-cloned, and sequenced to look for disruption of the *Rag2* gene. Out of 76 sequenced clones, 2 clones had deletions in the *Rag2* gene (Fig. 1B). One clone contained a single-nucleotide deletion, and a second clone contained a two-nucleotide deletion. Six other clones contained point mutations within the targeted region.

Genome-modified spermatogonia express stemness marker

Spermatogonia were expanded until passage 16 (4.5 months in culture) for nucleofection to introduce the genetic mutations. To confirm that these spermatogonia maintained their stemness and chromosomal integrity, we analyzed the expression of ZBTB16 (*PLZF*), which is a marker for mammalian type A spermatogonia and has been shown to be critical for SSC self-renewal (40, 41). MEFs did not express ZBTB16, whereas fresh SSCs did (Fig. 2A). SD-WT2 spermatogonia showed consistent and robust expression of ZBTB16 even after being expanded to passage 16 over a 5-month culture period (Fig. 2B). Spermatogonia at passage 16 were also sent to IDEXX for karyotype analysis, which verified that these SSCs did not

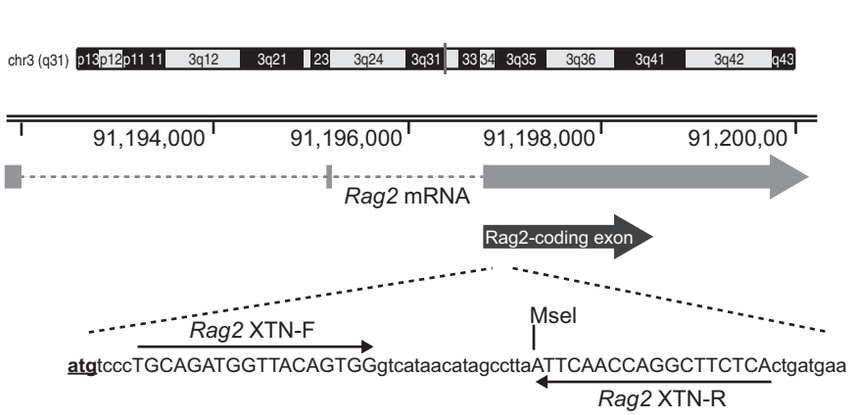

B

E10	**atg**tcccTGCAGATGGTTACAGTGGgtcataac-tagccttaATTCAACCAGGCTTCTCA
G03	**atg**tcccTGCAGATGGTTACAGTGGgtcataacat**g**gccttaATTCAACCAGGCTTCTCA
B10	**atgc**cccTGCAGATGGTTACAGTGGgtcataacatagccttaATTCAACCAGGCTTCTCA
E05	**atg**tcccTGCAGAT**A**GTTACAGTGGgtcataacatagccttaATTCAACCAGGCTTCTCA
D04	**atg**tcccTGCAGATGGTTACAGTGGgtcataacatagccttaATTCAACC**C**GGCTTCTCA
A12	**atg**tccc**C**GCAGATGGTTACAGTGGgtcataacatagccttaATTCAACCAGGCTTCTCA
F02	**atg**tc**t**cTGCAGATGGTTACAGTGGgtcataacatagccttaATTCAACCAGGCTTCTCA
A05	**atg**tcccTGCAGATGGTTACAGTGGgtcata- -atagccttaATTCAACCAGGCTTCTCA
B02	**atg**tcccTGCAGATGGTTACAGTGGgtcataacatagccttaA**C**TCAACCAGGCTTCTCA
REF	**atg**tcccTGCAGATGGTTACAGTGGgtcataacatagccttaATTCAACCAGGCTTCTCA

Figure 1.
Disruption of *Rag2* gene in rat SSCs. **A,** The XTN pair targets early in the single-coding exon of *Rag2* gene. XTN-binding sites are capitalized, the *Rag2* start codon is shown in boldface font and underlined, and the MseI site utilized for genotyping is marked. **B,** Alignment of clones to the wild-type reference sequence. Reference sequence is underlined, the XTN-binding sites are shown in uppercase, mutations are shown in bold font, and *Rag2* start codon is in bold font and underlined. Clone E10 contains a single-nucleotide deletion, and clone A05 contains a two-nucleotide deletion.

contain any chromosomal anomalies (Supplementary Fig. S1A and S1B).

SDR rat

The pool of spermatogonia containing 3% modified SSCs was transplanted into seminiferous tubules (35, 36) of four busulfan-treated *Dazl*-deficient rats. At approximately 80 days after transplantation, recipient males were paired with wild-type females. All modified SSCs were transplanted into recipient rats within 3 hours of their thawing. Three out of the four recipients had greater than 50% fill in at least one of their testes, with two also showing signs of bleeding during transplantation surgery. The recipient that had a high fill percentage and no bleeding during transplantation produced pups (Table 1). The recipient sired 8 litters with a total of 60 pups. The pups were screened for loss of the targeted MseI site by subjecting the amplified locus to MseI digestion. As shown in Fig. 3A, 1 out of the 60 pups (2f) was identified to carry a disrupted allele. Sequencing analysis revealed this allele to be a 27 bp deletion mutant. The allele was then bred to homozygosity to generate the SDR rat. Thymus and spleen were collected from SDR rat, and Western blot was performed to determine *Rag2* protein expression using a *Rag2* antibody. Because the SDR rat carries an in-frame 27 bp deletion mutation in the Rag2 gene, Western blot analysis showed similar expression of the *Rag2* protein in the SDR and wild-type rats (Supplementary Fig. S2).

SDR rat lacks mature B- and T-cell populations

Splenocytes and thymocytes were collected from age-matched wild-type and homozygous mutant animals and analyzed by flow cytometry to characterize the immune cell populations in the SDR rat. Homozygous mutant animals were essentially athymic with residual tissue equating to less than 10% the weight of thymus tissue in the wild-type. Mature T cells were identified by double staining for T-cell antigens CD4 and CD8 (32, 42). The SDR thymocyte population contained only 7.55% $CD4^+/CD8^+$ cells and 81% $CD4^-/CD8^-$ cells (Fig. 4A, right plot), drastically reduced from the wild-type thymocyte population, which consisted of 89.24% $CD4^+/CD8^+$ cells and less than 2% $CD4^-/CD8^-$ cells (Fig. 4B, left plot).

Mature B cells were identified as double-positive B220/IgM population of splenocytes (32, 43). The spleens from homozygous mutant animals were smaller compared with the wild-type spleen. In a *Rag2*-null genotype, the B-cell receptor genes should not be capable of V(D)J recombination. Thus, as expected, the SDR rats had no B220/IgM double-positive splenocytes (Fig. 4B, right plot).

Interestingly, the SDR rat had an increase in NK cells compared with the wild-type rat. Whereas the wild-type rat has 3.97% NK cells in the splenocytes and less than 1% NK cells in the thymocyte population (Fig. 4C, left plots), the SDR rat splenocytes and thymoctyes contained 43.94% and 5.41% NK cells, respectively (Fig. 4C and D, right plots). The increase in NK cells seen in our SDR rats is similar to that seen in a *Rag1* knockout rat (17), a different *Rag2* knockout rat (44), the *Prkdc* SCID rat which lacks mature B and T cells (45), and the SCID mouse. In addition, *Rag2*-null mice exhibit greater NK-cell activity than their wild-type littermates (32). Although we do not know the mechanism resulting in the increased NK cells, these published data suggest this is a common phenomenon among immunodeficient animals lacking mature T and B cells.

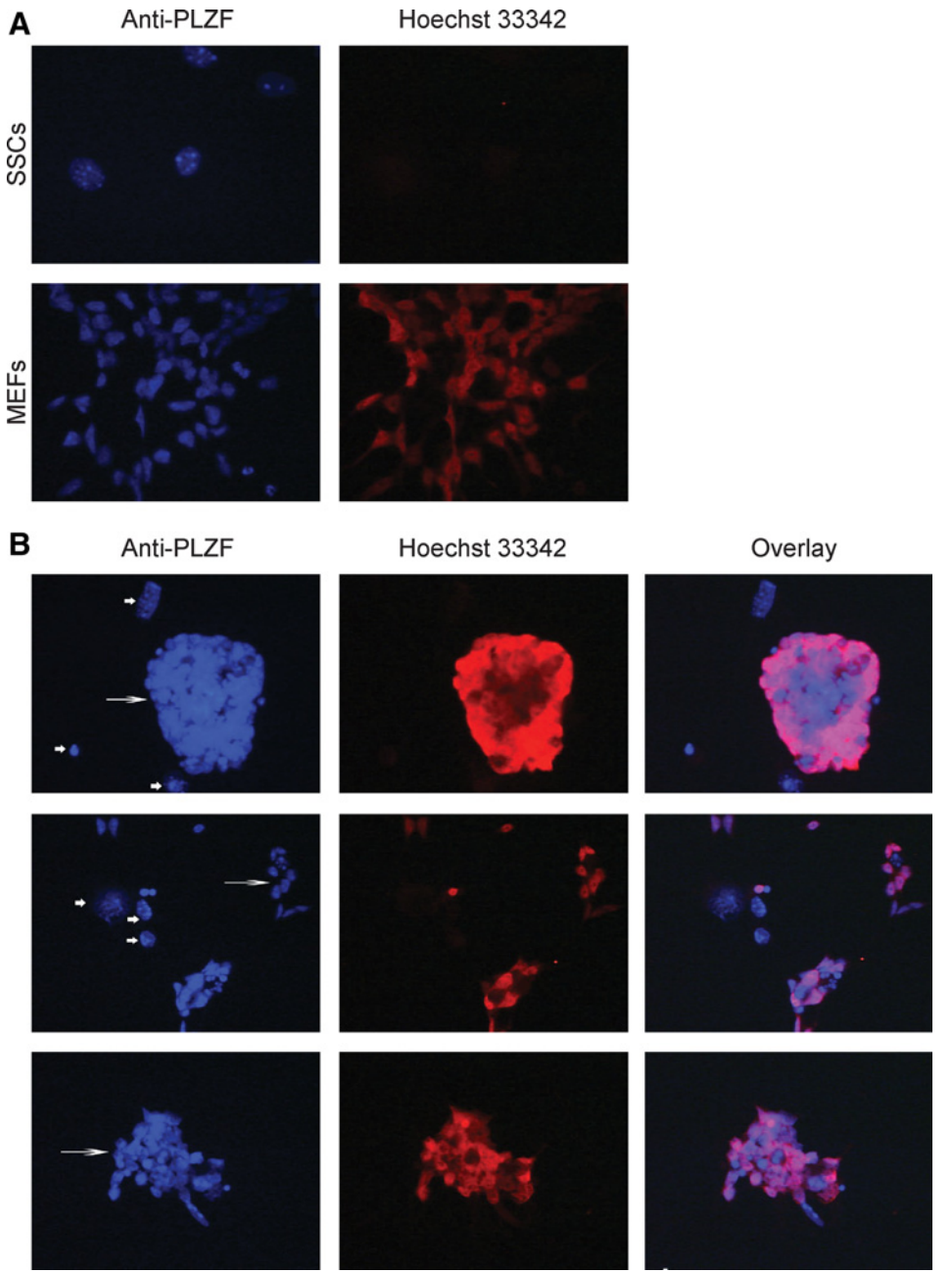

Figure 2.
Expression of ZBTB16 (PLZF) in MEFs, fresh SSCs, and parental SD-WT2 SSCs kept in culture for 4.5 months (passage 16). Cells were stained with anti-PLZF antibody (red) and Hoechst 33342 (blue). **A,** Fresh SSCs (passage 9) on laminin show undifferentiated spermatogonia that express ZBTB16 (PLZF), whereas the MEFs do not. **B,** Immunocytochemistry of SSC clusters at passage 16 on feeders. First column with Hoechst33342 nuclear staining shows SSCs (long arrow) and feeders (short arrow). Second column shows PLZF staining. Third column shows merged images of PLZF staining and Hoechst33342.

Table 1. Production of SDR rats by implanting *Rag2* SSCs into sterile males

Animal ID	Time from thaw to transplant	Right testis (fill %)	Left testis (fill %)	Surgery outcome	Days to mating	Days to 1st litter	Total pups screened	*Rag2* pups
526308	0.75 h	20	10	Good	77	n/a	n/a	n/a
526300	1.6 h	15	90	Good	81	142	60	1
526309	2 h	60	100	Survived, but was bleeding during surgery	70	n/a	n/a	n/a
526310	2.75 h	Miss	75	Survived, but was bleeding during surgery	70	n/a	n/a	n/a

NOTE: Four recipient males were transplanted with genetically modified SSCs. Only one recipient (526300) had no surgical complications and had good fill of testis with modified SSCs. Only that recipient produced pups when mated with wild-type females.

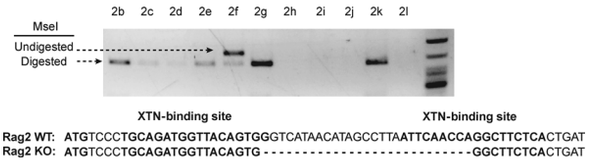

Figure 3.

Genotyping pups for disruptions in *Rag2* gene. The targeted locus was amplified from pups sired by the implanted male and subjected to MseI digestion. Animal 2f contained at least one allele that is resistant to MseI digestion (white arrow). The PCR product from animal 2f was TOPO cloned and sequenced which revealed this animal carries a mutant allele with a 27 bp deletion.

Analysis of SDR whole blood demonstrated greatly diminished T and B cells compared with the wild-type rat (Supplementary Fig. S3A–S3C). The wild-type rat has a significant population of circulating $CD4^+$, $CD8^+$, and CD4/CD8 double-positive T-cell populations compared with the SDR rat (Supplementary Fig. S3A). The wild-type rat has over 20% B220/IgM double-positive mature B cells, compared with 3.5% in the SDR rat (Supplementary Fig. S3B). Interesting, the SDR rat has slightly less circulating NK cells, unlike what is observed in the spleen (Supplementary Fig. S3C).

Subcutaneous human glioblastoma tumor growth

To determine if the SDR rat was permissive for human cancer xenotransplantation, we transplanted a human glioblastoma

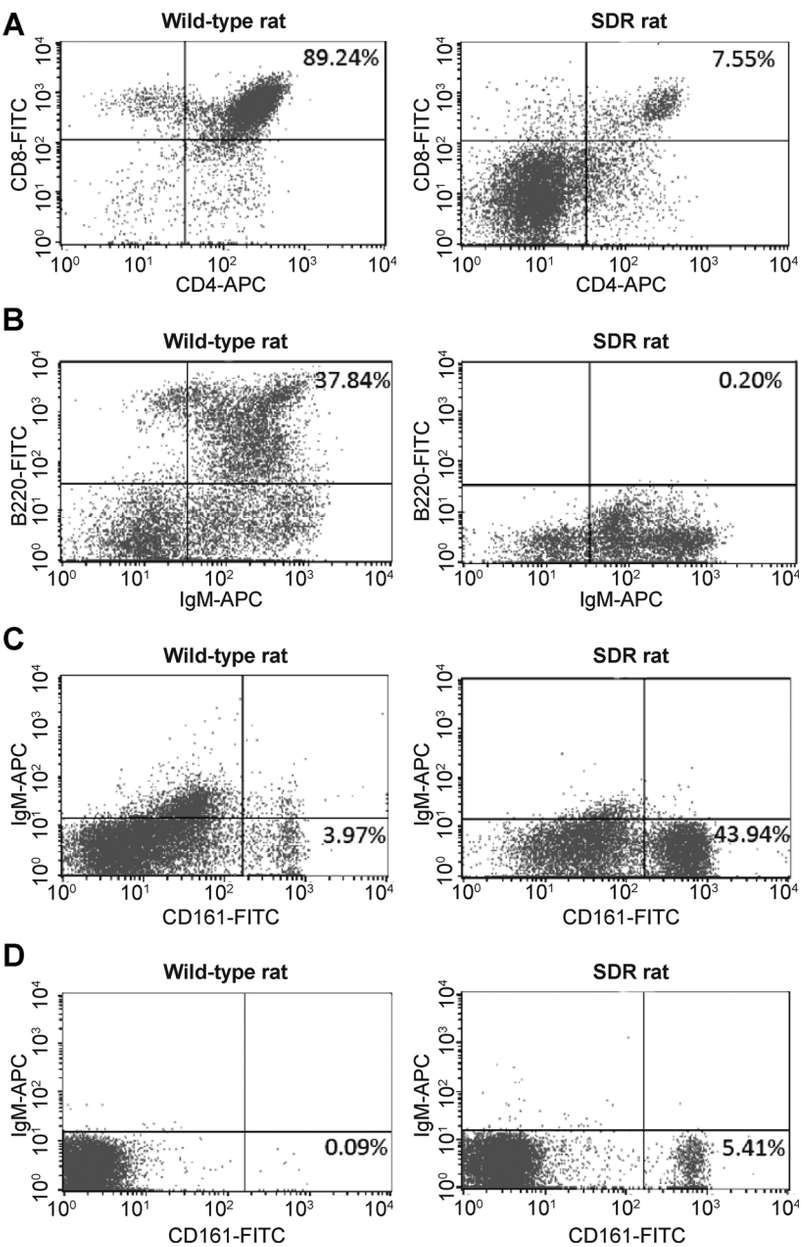

Figure 4.

Immunophenotyping of the SDR rat. **A,** SDR thymocytes contain only 7.55% $CD4^+/CD8^+$ mature T cells (right plot), compared with 89.24% in a wild-type control (left plot). The majority of thymocytes are CD4 and CD8 double negative in the SDR rat. **B,** The SDR rat spleen contains no mature B cells as demonstrated by lack of $B220^+/IgM^+$ cells (right plot), whereas the wild-type spleen contains 37.84% $B220^+/IgM^+$ mature B cells (left plot). **C** and **D,** SDR rat spleen (**C**) and thymus (**D**) have an increased NK-cell population (43.94% and 5.41%, respectively) compared with only 3.97% in the wild-type spleen (**C**) and less than 1% in the wild-type thymus. Left plots: wild-type rat. Right plots: SDR rat.

cell line (U87MG) subcutaneously into 6 SDR rats, 2 *Rag2* heterozygous rats, and 1 wild-type rat. The cells were resuspended in Geltrex prior to inoculation to provide structural support for cell survival and growth. No tumors grew during the study period in the wild-type and heterozygous animals. All 6 SDR rats showed subcutaneous tumor growth (Fig. 5A), detectable as early as 10 days after injection. All tumors reached the maximum allowable size of 40 mm diameter by 49 days after injection (Fig. 5B). The tumors all stained positive for the human mitochondrial protein (Fig. 5C). Tissue from a rat that had not been injected with human cells did not show positive staining with the antibody (Fig. 5C).

SDR rat is a suitable model for human xenograft studies

In the second study, a KRAS-mutant NSCLC cell line H358 was implanted into the SDR rat subcutaneously. Tumor growth was observed and compared with growth in nude (nu/nu) and NSG mice. Note that 1×10^6, 5×10^6, or 1×10^7 cells were implanted in the SDR rat, whereas 1×10^7 cells were implanted in the nude and NSG mice. The engraftment rate was 100% in the SDR rat for all three cell-densities implanted, and growth rate was directly proportional to the amount of cells transplanted. In addition, the tumors grew much faster and more consistently in the SDR rat than in the mouse models (Fig. 6A; Supplementary Table S1).

In a pilot study performed to further explore the ability of the SDR rat to accommodate patient primary tumor-derived cell lines, human ovarian cancer (OV81; ref. 46) and human endometrial cancer (OV185) xenografts were established in the flanks of female SDR rats by implanting 2×10^6 cells of OV81 and OV185 in to 3 SDR rats each. Tumors implanted with OV81 cells showed 100% engraftment rate with rapid tumor uptake in as early as 8 days and consistent growth kinetics (Fig. 6B). In SDR rats implanted with OV185 cells, the tumor engraftment rate was 66.7% (2/3 rats engrafted) with consistent growth kinetics and tumors detectable in 6 to 8 days (Fig. 6C). One rat did not engraft the tumor, and we attribute this to a technical problem with the implantation.

Discussion

Despite its central role in toxicologic, pharmacologic, neurobehavioral, and physiologic studies, rats have lagged far behind the mouse as a genetic model (14). We have created a rat with a mutation in the *Rag2* gene resulting in a complete lack of mature B cells and significantly reduced mature T-cell population. Although targeting the *Rag2* locus resulted in an in-frame deletion that does not alter *Rag2* protein levels, the lack of mature B and T cells in the rats suggests that the deletion results in a nonfunctional protein. The mechanism has not been determined.

Several immunodeficient mouse strains exist, exhibiting a range of immune phenotypes, all with differing capabilities for accepting various human cell types for xenograft studies. No two immunodeficient mouse strains are alike. However, until recently, with the discovery of TALENs and CRISPR/Cas9 technology, the only immunodeficient rat strain in existence was the Nude rat (RNU; NIH-*Foxn1*^{rnu}), which only lacks mature T cells. Although the Nude rat has been useful for some human xenograft studies, there are far less human cancer cell lines with survival and growth data in the rat compared with the plethora of cell lines that have been able to be modeled in the mouse. Still, there are some human cancer cell lines that have not been successfully grown in any immunodeficient mouse model. It is possible that these cell lines will

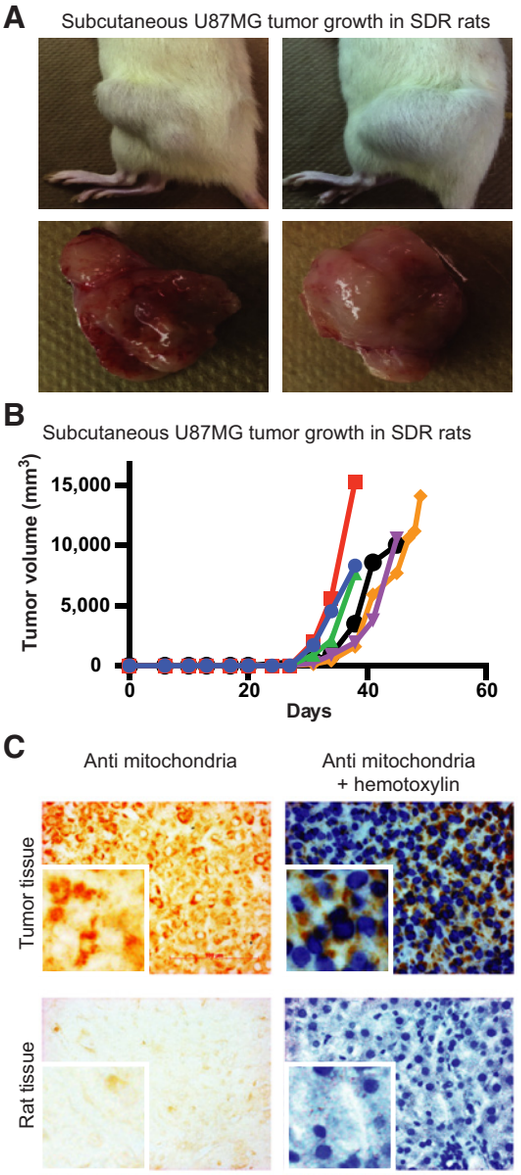

Figure 5.
Subcutaneous growth of human glioblastoma U87MG cells in the SDR rat. Note that 1×10^6 U87MG cells resuspended in Geltrex were injected subcutaneously into SDR rats. **A,** Tumor growth in two different SDR animals with images of their excised tumors. **B,** Tumor volume (mm^3) over time. Each line represents tumor growth in an individual rat. **C,** Immunohistochemistry of anti–human-mitochondria in tumor tissue and rat tissue. Brown staining demonstrates perinuclear localization of human-mitochondria protein in a tumor section, with (right) and without (left) hematoxylin counterstain. Magnification, x40. The antibody for human mitochondria protein does not show staining in tissue from a rat that was not injected with human cells (negative control). Right plot with hematoxylin counterstain; magnification, x40; scale bar, 100 μm.

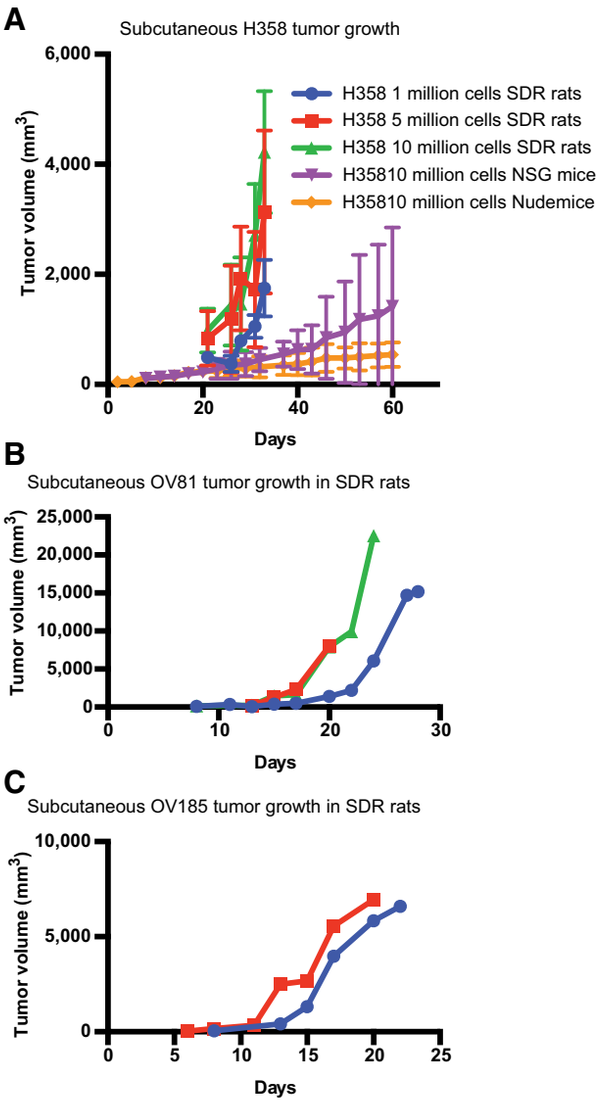

Figure 6.

Subcutaneous tumor growth of NSCLC, ovarian, and endometrial cells in SDR rats. **A,** H358 cancer cells were transplanted subcutaneously in the SDR rat. Three groups of six rats received either 1×10^6, 5×10^6, or 1×10^7 cells in 5 mg/mL Geltrex. In comparison, 1×10^7 H358 cells were injected in 6 nude and 6 NSG mice, and growth was tracked for 60 days. Average tumor growth (mm^3) over time. **B,** 2×10^6 OV81 cells resuspended in 5 mg/mL Geltrex were injected subcutaneously into 3 female SDR rats. Graph shows three individual rat tumor volumes over time (mm^3). Each line represents tumor growth in an individual rat. **C,** 2×10^6 OV185 cells resuspended in 5 mg/mL Geltrex were injected subcutaneously into 2 female SDR rats. Graph shows two individual rat tumor volumes over time (mm^3). Each line represents tumor growth in an individual rat.

not be rejected in a different immunodeficient species, such as the rat.

Here, we show proof of principle for human xenograft capabilities for our immunocompromised rat. SDR rat demonstrated efficient uptake and tumor growth kinetics for a wide range of human cancer types. For the NSCLC cell line H358, SDR rat demonstrated superior uptake rate than the NSG mouse—which is the gold standard for human xenograft models. Furthermore, the H358 xenografts grew much more uniformly with far less variance in the SDR rat compared with the NSG mouse. In our pilot studies with PDX-derived ovarian (OV81) and endometrial (OV185) cell lines, SDR rats also demonstrated a rapid tumor uptake and consistent growth kinetics, with faster growth to much larger tumor sizes than seen in mice.

Although our data demonstrate that this SDR rat can accept human xenografts, it is possible that the increase in NK cells will impede engraftment of other human cell types. For this reason, we have created another genetically modified rat with depleted NK cells in addition to the loss of mature T and B cells. This rat strain will potentially support the growth of more human cell types. This model is currently being characterized and validated for its ability to support the growth of human cells.

Disclosure of Potential Conflicts of Interest

E. Ostertag is CEO at Transposagen Biopharmaceuticals Inc., is Director at Hera BioLabs Inc., and has an ownership interest (including stock, patents, etc.) in Transposagen Biopharmaceuticals, Inc. and Hera BioLabs Inc. G. Narla has an ownership interest (including stock, patents, etc.) in RAPPTA Therapeutics and is a consultant/advisory board member for HERA biosciences. T.Y. Jamling is VP of R&D at, and has an ownership interest (including stock, patents, etc.) in, Hera Testing Laboratories Inc. No potential conflicts of interest were disclosed by the other authors.

Authors' Contributions

Conception and design: F.K. Noto, V. Adjan-Steffey, E. Ostertag, J. Crawford, G. Narla, T.Y. Jamling

Development of methodology: V. Adjan-Steffey, A. Arey, C.B. McClain, E. Ostertag, G. Narla, T.Y. Jamling

Acquisition of data (provided animals, acquired and managed patients, provided facilities, etc.): F.K. Noto, V. Adjan-Steffey, M. Tong, K. Ravichandran, W. Zhang, A. Arey, C.B. McClain, S. Mazhar, A. DiFeo, T.Y. Jamling

Analysis and interpretation of data (e.g., statistical analysis, biostatistics, computational analysis): F.K. Noto, V. Adjan-Steffey, K. Ravichandran, W. Zhang, E. Ostertag, S. Mazhar, J. Sangodkar, A. DiFeo, G. Narla, T.Y. Jamling

Writing, review, and/or revision of the manuscript: F.K. Noto, V. Adjan-Steffey, K. Ravichandran, J. Sangodkar, J. Crawford, G. Narla, T.Y. Jamling

Administrative, technical, or material support (i.e., reporting or organizing data, constructing databases): V. Adjan-Steffey, M. Tong, K. Ravichandran, A. Arey, G. Narla, T.Y. Jamling

Study supervision: F.K. Noto, V. Adjan-Steffey, E. Ostertag, G. Narla, T.Y. Jamling

Acknowledgments

We thank Dr. Bjoern Bauer at the University of Kentucky for the gift of the human glioblastoma cell. All tissue processing, embedding, and sectioning were performed by the University of Kentucky Imaging Core Facility. Histology and immunohistochemistry imaging was done using equipment at the University of Kentucky Imaging Core Facility. Flow cytometry analysis was performed by the University of Kentucky Flow Cytometry Core.

This study was supported by KSTC-18451217249 [T.Y. Jamling (PI, alias: T. Yeshi), F.K. Noto, W. Zhang, A. Arey, C.B. McClain, and J. Crawford] and R44GM099206 [E. Ostertag (PI) and T.Y. Jamling].

The costs of publication of this article were defrayed in part by the payment of page charges. This article must therefore be hereby marked *advertisement* in accordance with 18 U.S.C. Section 1734 solely to indicate this fact.

Received February 8, 2018; revised July 10, 2018; accepted September 5, 2018; published first September 11, 2018.

References

1. Anderson S, Luffer-Atlas D, Knadler MP. Predicting circulating human metabolites: how good are we? Chem Res Toxicol 2009;22:243–56.
2. Leclercq L, Cuyckens F, Mannens GS, de Vries R, Timmerman P, Evans DC. Which human metabolites have we MIST? Retrospective analysis, practical aspects, and perspectives for metabolite identification and quantification in pharmaceutical development. Chem Res Toxicol 2009;22:280–93.
3. Walker D, Brady J, Dalvie D, Davis J, Dowty M, Duncan JN, et al. A holistic strategy for characterizing the safety of metabolites through drug discovery and development. Chem Res Toxicol 2009;22:1653–62.
4. Peltz G. Can `humanized' mice improve drug development in the 21st century? Trends Pharmacol Sci 2013;34:255–60.
5. Mak IW, Evaniew N, Ghert M. Lost in translation: animal models and clinical trials in cancer treatment. Am J Transl Res 2014;6:114–8.
6. Xu D, Peltz G. Can humanized mice predict drug "behavior" in humans? Annu Rev Pharmacol Toxicol 2016;56:323–38.
7. Fattinger K, Funk C, Pantze M, Weber C, Reichen J, Stieger B, et al. The endothelin antagonist bosentan inhibits the canalicular bile salt export pump: a potential mechanism for hepatic adverse reactions. Clin Pharmacol Ther 2001;69:223–31.
8. Manning F, Swartz M. Review of the Fialuridine (FIAU) clinical trials. Washington, DC: Institute of Medicine (US); 1995.
9. McKenzie R, Fried MW, Sallie R, Conjeevaram H, Di Bisceglie AM, Park Y, et al. Hepatic failure and lactic acidosis due to fialuridine (FIAU), an investigational nucleoside analogue for chronic hepatitis B. N Engl J Med 1995;333:1099–105.
10. Shultz LD, Goodwin N, Ishikawa F, Hosur V, Lyons BL, Greiner DL. Human cancer growth and therapy in immunodeficient mouse models. Cold Spring Harb Protoc 2014;2014:694–708.
11. Gad S. (Ed.). (2006). Animal models in toxicology. Boca Raton: CRC Press.
12. Jacob HJ. Functional genomics and rat models. Genome Res 1999;9:1013–6.
13. Iannaccone PM, Jacob HJ. Rats! Dis Model Mech 2009;2:206–10.
14. Lazar J, Moreno C, Jacob HJ, Kwitek AE. Impact of genomics on research in the rat. Genome Res 2005;15:1717–28.
15. Mollard S, Mousseau Y, Baaj Y, Richard L, Cook-Moreau J, Monteil J, et al. How can grafted breast cancer models be optimized? Cancer Biol Ther 2011;12:855–64.
16. Nofiele JT, Cheng HL. Establishment of a lung metastatic breast tumor xenograft model in nude rats. PLoS One 2014;9:e97950.
17. Tsuchida T, Zheng YW, Zhang RR, Takebe T, Ueno Y, Sekine K, et al. The development of humanized liver with Rag1 knockout rats. Transplant Proc 2014;46:1191–3.
18. Ménoret S, Fontanière S, Jantz D, Tesson L, Thinard R, Rémy S, et al. Generation of Rag1-knockout immunodeficient rats and mice using engineered meganucleases. FASEB J 2013;27:703–11.
19. Festing MF, May D, Connors TA, Lovell D, Sparrow S. An athymic nude mutation in the rat. Nature 1978;274:365–6.
20. Colston MJ, Fieldsteel AH, Dawson PJ. Growth and regression of human tumor cell lines in congenitally athymic (rnu/rnu) rats. J Natl Cancer Inst 1981;66:843–8.
21. Drewinko B, Moskwa P, Lotzovà E, Trujillo JM. Successful heterotransplantation of human colon cancer cells to athymic animals is related to tumor cell differentiation and growth kinetics and to host natural killer cell activity. Invasion Metastasis 1986;6:69–82.
22. Maruo K, Ueyama Y, Kuwahara Y, Hioki K, Saito M, Nomura T, et al. Human tumour xenografts in athymic rats and their age dependence. Br J Cancer 1982;45:786–9.
23. Fowler JA, Mundy GR, Lwin ST, Lynch CC, Edwards CM. A murine model of myeloma that allows genetic manipulation of the host microenvironment. Dis Model Mech 2009;2:604–11.
24. Belizário JE. Immunodeficient mouse models: an overview. The Open Immunology Journal 2009;2:79–85.
25. Holzapfel BM, Wagner F, Thibaudeau L, Levesque JP, Hutmacher DW. Concise review: humanized models of tumor immunology in the 21st century: convergence of cancer research and tissue engineering. Stem Cells 2015;33:1696–704.
26. Mazurier F, Fontanellas A, Salesse S, Taine L, Landriau S, Moreau-Gaudry F, et al. A novel immunodeficient mouse model–RAG2 x common cytokine receptor gamma chain double mutants–requiring exogenous cytokine administration for human hematopoietic stem cell engraftment. J Interferon Cytokine Res 1999;19:533–41.
27. van Rijn RS, Simonetti ER, Hagenbeek A, Hogenes MC, de Weger RA, Canninga-van Dijk MR, et al. A new xenograft model for graft-versus-host disease by intravenous transfer of human peripheral blood mononuclear cells in RAG2-/- gammac-/- double-mutant mice. Blood 2003;102:2522–31.
28. Ishikawa F, Yasukawa M, Lyons B, Yoshida S, Miyamoto T, Yoshimoto G, et al. Development of functional human blood and immune systems in NOD/SCID/IL2 receptor {gamma} chain(null) mice. Blood 2005;106:1565–73.
29. Stevens LC, Little CC. Spontaneous testicular teratomas in an inbred strain of mice. Proc Natl Acad Sci U S A 1954;40:1080–7.
30. Thomas KR, Capecchi MR. Site-directed mutagenesis by gene targeting in mouse embryo-derived stem cells. Cell 1987;51:503–12.
31. Tasher D, Dalal I. The genetic basis of severe combined immunodeficiency and its variants. Appl Clin Genet 2012;5:67–80.
32. Shinkai Y, Rathbun G, Lam KP, Oltz EM, Stewart V, Mendelsohn M, et al. RAG-2-deficient mice lack mature lymphocytes owing to inability to initiate V(D)J rearrangement. Cell 1992;68:855–67.
33. Chapman KM, Medrano GA, Jaichander P, Chaudhary J, Waits AE, Nobrega MA, et al. Targeted germline modifications in rats using CRISPR/Cas9 and spermatogonial stem cells. Cell Rep 2015;10:1828–35.
34. Wu Z, Falciatori I, Molyneux LA, Richardson TE, Chapman KM, Hamra FK. Spermatogonial culture medium: an effective and efficient nutrient mixture for culturing rat spermatogonial stem cells. Biol Reprod 2009;81:77–86.
35. Izsvák Z, Fröhlich J, Grabundzija I, Shirley JR, Powell HM, Chapman KM, et al. Generating knockout rats by transposon mutagenesis in spermatogonial stem cells. Nat Methods 2010;7:443–5.
36. Ivics Z, Izsvák Z, Chapman KM, Hamra FK. Sleeping Beauty transposon mutagenesis of the rat genome in spermatogonial stem cells. Methods 2011;53:356–65.
37. Tomayko MM, Reynolds CP. Determination of subcutaneous tumor size in athymic (nude) mice. Cancer Chemother Pharmacol 1989;24:148–54.
38. Reyon D, Tsai SQ, Khayter C, Foden JA, Sander JD, Joung JK. FLASH assembly of TALENs for high-throughput genome editing. Nat Biotechnol 2012;30:460–5.
39. Reyon D, Maeder ML, Khayter C, Tsai SQ, Foley JE, Sander JD, et al. Engineering customized TALE nucleases (TALENs) and TALE transcription factors by fast ligation-based automatable solid-phase high-throughput (FLASH) assembly. Curr Protoc Mol Biol 2013;Chapter 12:Unit 12.6.
40. Costoya JA, Hobbs RM, Barna M, Cattoretti G, Manova K, Sukhwani M, et al. Essential role of Plzf in maintenance of spermatogonial stem cells. Nat Genet 2004;36:653–9.
41. Buaas FW, Kirsh AL, Sharma M, McLean DJ, Morris JL, Griswold MD, et al. Plzf is required in adult male germ cells for stem cell self-renewal. Nat Genet 2004;36:647–52.
42. Bruno L, Res P, Dessing M, Cella M, Spits H. Identification of a committed T cell precursor population in adult human peripheral blood. J Exp Med 1997;185:875–84.
43. Kövesdi D, Bell SE, Turner M. The development of mature B lymphocytes requires the combined function of CD19 and the p110δ subunit of PI3K. Self Nonself 2010;1:144–53.
44. Liu Q, Fan C, Zhou S, Guo Y, Zuo Q, Ma J, et al. Bioluminescent imaging of vaccinia virus infection in immunocompetent and immunodeficient rats as a model for human smallpox. Sci Rep 2015;5:11397.
45. Mashimo T, Takizawa A, Kobayashi J, Kunihiro Y, Yoshimi K, Ishida S, et al. Generation and characterization of severe combined immunodeficiency rats. Cell Rep 2012;2:685–94.
46. Nagaraj AB, Joseph P, Kovalenko O, Singh S, Armstrong A, Redline R, et al. Critical role of Wnt/β-catenin signaling in driving epithelial ovarian cancer platinum resistance. Oncotarget 2015;6:23720–34.